Communications on Applied Nonlinear Analysis
ISSN: 1074-133X
Vol 32 No. 2 (2025)

Validation of Size of Semiconductor Nano Material: Effect on Size and Shape

Dr H V Ganvir[1], Bathula Jonathan [2], K Sangeet Kumar [3], Vadali Pitchi Raju [4], Prabhakaran K [5], Prajwal Hegde N [6]

[1]Department of Applied Physics, Yeshwantrao Chavan College of Engineering, Nagpur, India. hrwasnik@gmail.com

[2]Department of CSE, KONERU LAKSHMAIAH EDUCATION FOUNDATION (KL Deemed university), Vaddeswaram, Guntur, Andhra Pradesh, India. jonathanbathula20@gmail.com

[3] Department of Electronics and Communication Engineering, Aditya college of Engineering and Technology, Aditya Nagar, ADB Road, Surampalem, East-Godavari District, Andhra Pradesh, India. sangeetkumar_ece@acoe.edu.in

[4]Department of Mechanical Engineering, Indur Institute of Engineering & Technology, Ponnala Road, Siddipet, Medak, Telangana, India. vpraju2000@gmail.com

[5]Center for Environmental Research, Department of Chemistry, Kongu Engineering College, Perundurai , Erode, Tamil Nadu, India. prabhakaranchemist@gmail.com

[6] Department of Artificial Intelligence and Data Science, NMAM Institute of Technology (NMAMIT),Nitte (Deemed to be University), Karkala ,India. prajwal.hegde@nitte.edu.in

Article History:

Received: *27-07-2024*

Revised: *05-09-2024*

Accepted: *17-09-2024*

Abstract:

A formulation is provided for the band gap energy of semiconductor compound nanomaterials (SCNs), which is dependent on their size and shape. The theoretical model is based upon the measure of cohesive energy shown by nanocrystals in relation to bulk crystals. The investigation of size- and shape-dependent band gap energy has been conducted on semiconductor compounds including CdSe, CdTe, ZnS, ZnSe, and ZnTe. Band gap energy of single-crystal nanoparticles (SCN) is determined by the size and form of the particles. Based on the model, it is predicted that the band gap energy of semiconductor nanomaterials rises as their particle size decreases. This study compares the generated findings with the existing experimental data, which confirm the accuracy of the provided model.

Keywords: Formulation, semiconductor, size and shape, SCN, band gap.

1. Introduction

The scientific world has seen a significant surge in research on semiconductor nanoparticles owing to their distinct mechanical, optical, photonic, and electrical characteristics. [1-4] With the aid of the Wein2K code, they have recently reported on the mechanical, structural, electrical, magnetic, and optical behaviours in Zn1–xMnxS ($0 \leq x \leq 1$). Characterising the qualities of nanomaterials is largely dependent on their surface area to volume ratio, which affects several of these attributes. [5-8] A semiconductor's band gap is one of its most significant and essential characteristics. Electrical and optical characteristics of semiconductor materials are fundamentally influenced by band gaps. [9-14] To have a better understanding of their features, it is thus important and crucial to investigate the SCN's band gap growth. The large band gap of semiconductors makes them useful in a variety of applications. The indirect and tiny band gap of bulk silicon limits its utilisation, although Si photon nanodevices have been manufactured and utilised extensively. Numerous theoretical and experimental researchers have taken a size-dependent band gap stance. [15-17] With the use of photoluminescence spectra, the

diameter dependency of the effective band gaps in the wires is calculated and compared to the predictions of several theoretical models as well as the practical findings for InAs quantum dots and rods. Barnard demonstrated that the individual diamond nanocrystals' shapes might provide a means of adjusting the band gap within the quantum confinement regime via the use of electronic structure simulations.

Atoms and holes in semiconductors at the nanoscale are confined because of the quantum confinement phenomenon. Consequently, the energy gap in the semiconductor widens or rises between the full and empty states. [18-20] This wider band gap impairs semiconductors' optical and electrical characteristics at the nanoscale in optoelectronic devices. Both photoluminescence and X-ray photoemission spectroscopy have been used in several investigations to determine the band gap value. Yet, the band gap of semiconductor compound nanomaterials (SCNs) is predicted theoretically, and it even has unique characteristics. There are currently no accepted theoretical models for the size- and shape-dependent band gap of semiconductor nanomaterials, despite the possibility of calculating the band gap in its whole without the need for approximations. [21-23] This work presents a theoretical model that proposes the size- and shape-dependent band gap energy of single-crystalline nanocrystals (SCNs) based on cohesive energy, without the need for modifiable parameters. Theoretical predictions are used to analyse the behaviour of CdSe, CdTe, ZnS, ZnSe, and ZnTe semiconductor group nanomaterials in spherical, nanowire, and nanofilm forms. [24] Study reveals that the size and form of particles may adjust the band gap energy of the single-crystal nanotube (SCN). Comparative analysis is conducted between the model predictions and the existing experimental data. [25] An excellent agreement confirms the soundness of our suggested model throughout the whole range of diameters. This model has the potential to be used in situations where there is a complete absence of experimental data.

2. Analysis theory

The total cohesive energy of the nanomaterial is defined as the energy resulting from the contributions of the surface and inner atoms, and it is stated as

$$E_{Total} = E_0(n - N) + \left(\frac{1}{2}\right) E_0 N, \qquad (1)$$

where n represents the aggregate atomic count in the nanosolid and N is the count of atoms on the metal surface. Hence, (n − N) represents the aggregate count of internal atoms inside the nanomaterial. E_0 is the specific cohesive energy of each atom in the bulk material. To calculate the cohesive energy per mole, formula Equation (1) may be expressed as

$$\mathrm{A}\frac{E_{Total}}{n} = AE_0\left(1 - \left(\frac{N}{n}\right)\right) + \left(\frac{1}{2n}\right) AE_0 N, \qquad (2)$$

where the number of Avogadro is A. In this case, AE_0 is the cohesive energy per mole of the matching bulk material (E_b), and $\mathrm{A}\frac{E_{Total}}{n}$ is the cohesive energy per mole of the nanomaterial E_n. Equation (2) may be substituted to get

$$E_n = E_b\left(1 - \left(\frac{N}{2n}\right)\right). \qquad (3)$$

Since the cohesive energy and melting temperature are said to be linearly related, we may express the relationship for the melting temperature of nanomaterials as

$$T_{mn} = T_{bm}\left(1 - \left(\frac{N}{2n}\right)\right). \quad (4)$$

The electrical conductivity σ (D, T), which is dependent on temperature and size, is represented using the Arrhenius formula as

$$\sigma\,(D,T) = \sigma_0 \exp\left(-\frac{E_a(D)}{k_B T}\right) \quad (5)$$

For nanocrystals, the pre-exponential constant σ_0 and the size-dependent activation energy for electrical migration, $E_a(D)$, are defined as $E_a(D) = E_c - E_F$, where E_c represents the conduction band energy and E_F represents the Fermi energy. By assuming that the electrical conductivity is unaffected by the melting temperature and size, it is possible to derive the equation σ (D, T_{mn}) = σ (bulk, T_{mb}), where T_{mn} and T_{mb} represent the melting temperatures of nanomaterials and large materials, respectively. Therefore, by using Equation (5), we get

$$\sigma_0(D)\exp\left(-\frac{E_a(D)}{k_B T_{mn}}\right) = \sigma_0(bulk) \times \exp\left(-\frac{E_a(bulk)}{k_B T_{mb}}\right)).$$

Ignoring the influence of size on σ0, we arrive at the equation $E_a(D)/E_a(bulk) = T_{mn}/T_{mb}$. Activation energy becomes $E_a = \frac{E_g}{2}$ because we know that, for most semiconductors, the Fermi level is located in the middle of the band gap. This suggests that the change in activation energy is proportionate to the change in energy band gap. As so, having the phrase that is more appropriate.

$$\frac{\Delta E_g(D)}{E_g(bulk)} = |\Delta E_a(D)/E_a(bulk)| \quad (6)$$

Where $\Delta E_g\ is\ a\ difference$ in energy band gap.

Or Equation (6) may be written as

$$\Delta\frac{E_g(D)}{E_g(bulk)} = |(E_a(D) - E_a(bulk)/E_a(bulk)|$$

Or

$$\frac{\Delta E_g(D)}{E_g(bulk)} = 1 - T_{mn}/T_{mb} \quad (7)$$

Using Eqn (4), Eqn (7) may be written as

$$E_g(D) = E_g(bulk)\left(1 + \frac{N}{2n}\right) \quad (8)$$

N/2n varies depending on the dimensions and morphology of the nanomaterials [19]. The equation N/2n for spherical nanosolids is equivalent to 2d/D, where d represents the diameter of an atom and D represents the diameter of the spherical nanosolids. The N/2n values for nanowire and nanofilm are 4d/3l and 2d/3h, respectively. These values are derived from the diameter of the nanowire (l) and the

breadth of the nanofilm (h). We get the following formulas by substituting the values of N/2n into Equation (8).

$$E_g(D) = E_g(bulk)\left(1 + \frac{2d}{D}\right) \quad (9)$$

$$E_g(I) = E_g(bulk)\left(1 + \frac{4d}{3I}\right) \quad (10)$$

$$E_g(h) = E_g(bulk)\left(1 + \frac{2d}{3h}\right) \quad (11)$$

For spherical nanosolids, nanowires, and nanofilms, respectively, the energy band gap is expressed by equations (9)– (11). In this work, the band gap energy shift of semiconductor compounds nanomaterials at various sizes and shapes is investigated using Equations (9)– (11).

3. Result and Discussion

To investigate how the size and structure of semiconductor nanoparticles affect the energy band gap, a simple model has been developed. Table 1 lists the input parameters needed for the theoretical computations.

Table. 1 Parameter input

Nanomaterials	E_g (bulk) eV	D(nm)
ZnS	3.69	0.235
ZnTe	2.38	0.188
CdSe	1.75	0.269
CdTe	1.45	0.286
ZnSe	2.8	0.255

Figures 1 through 12 present the collected results in conjunction with the available experimental data. Equation (9) for the size-dependent energy band gap of spherically shaped CdSe semiconductor nanoparticles is modelled and reported in Figure 1. Figure 1 displays comparisons between the expected outcomes and the experimental data that are currently available. The findings demonstrate that when particle size decreases, the band gap energy Eg(D) rises.

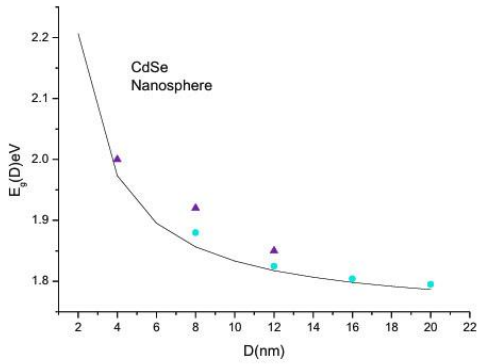

Figure.1 Effect of size on the energy band gap of CdSe nanospheres. The study's values derived using Equation (9) are displayed as continuous lines, whereas experimental data are shown as solid circles and triangles.

A significant rise in the value of Eg(D) is noticed when the particle size is smaller than 6 nm. Furthermore, spanning the whole range of the CdSe nanosphere, the expected outcomes coincide with the available experimental evidence. The quantum confinement theory, which postulates that the potential barriers of the surface or potential well of the quantum box confine the electrons in the conduction band and the holes in the valence band, also lends credence to our concept. As the particle size decreases, the band gap energy between the valence band and the conduction band rises due to the electron and hole confinement. Equation (10) yields the energy band gap of CdSe nanowire, which is shown in Figure 2 along with experimental evidence that validates the model's predictions. Figure 2 shows that when particle size decreases, the energy band gap widens. Starting at size 4 nm, there is a dramatic rise in the energy band gap.

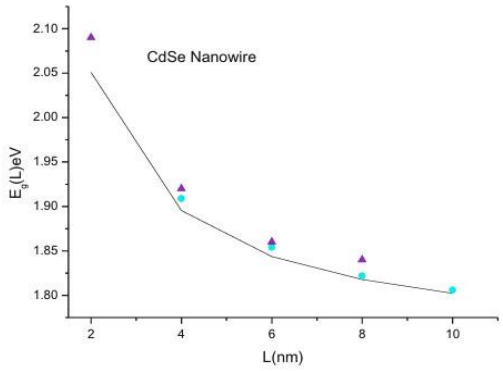

Figure.2 CdSe nanowire energy band gap varies with size. This study's Equation (10) values are illustrated by the continuous line, and the experimental findings are solid circles and triangles.

As shown in Figure 2, our findings closely resemble those of Li et al. The size-dependent energy band gap of semiconductor nanofilms made of CdSe, CdTe, ZnS, ZnSe, and ZnTe is determined using equation (11). The results of the computations are shown in Figures 3, 6, 9, and 12. It has been noted that as nanofilms become smaller, their energy band gap widens. The energy band gap increases with decreasing size, following the same pattern as spherical nanosolids and nanowires.

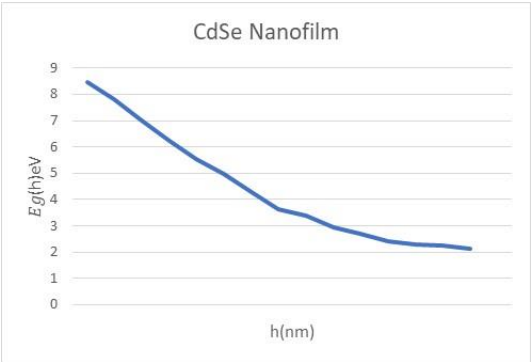

Figure.3 Effect of size on the energy band gap of CdSe nanofilm. The continuous line shows Equation (11) results from this investigation.

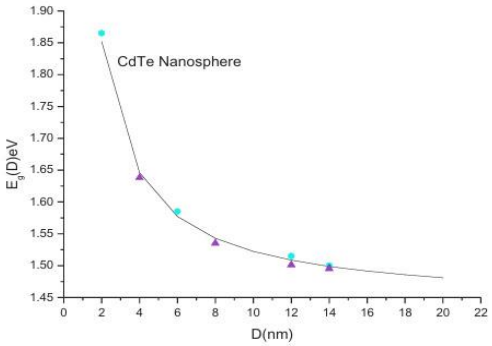

Figure.4 The energy band gap of CdTe nanospheres varies with size. In this research, values derived using Equation (9) are displayed as continuous lines, whereas experimental data are shown as solid circles and triangles.

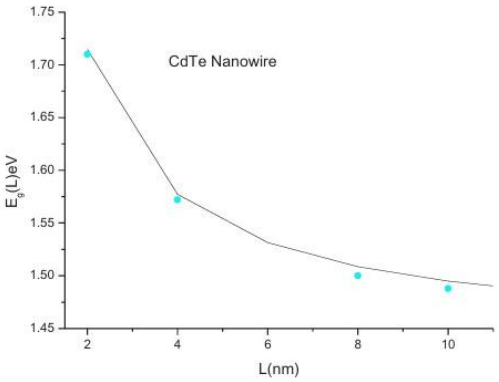

Figure.5 The energy band gap of CdTe nanowires varies with size. A continuous line shows the values estimated in this research using Equation (10) and solid circles indicate the experimental data.

Figure. 6 The energy band gap of CdTe nanofilm varies with size. This research determined values using Equation (11). The continuous line shows them.

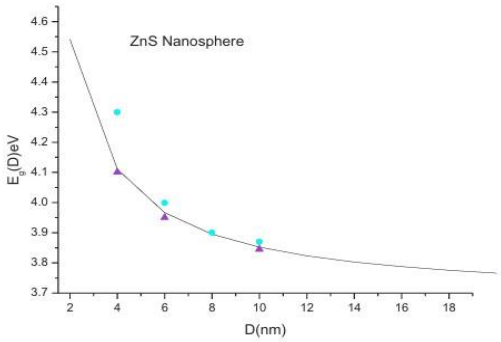

Figure.7 ZnS nanosphere energy band gap varies with size. In this research, Equation (9) values are illustrated by a continuous line, while experimental findings are solid circles and triangles.

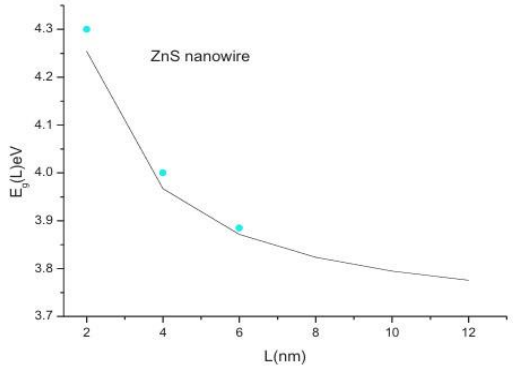

Figure.8 The energy band gap of ZnS nanowires varies with size. A continuous line shows the values estimated in this research using Equation (10) and solid circles indicate the experimental data.

Figure.9 The energy band gap of ZnS nanofilm varies with size. This research determined values using Equation (11). The continuous line shows them.

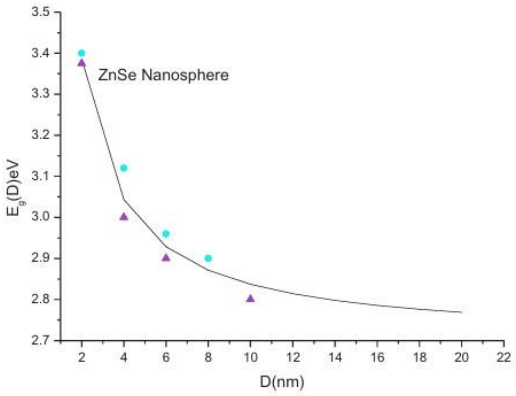

Figure.10 Variation in energy band gap of ZnSe nanospheres with size. The study's values derived using Equation (9) are displayed as continuous lines, whereas experimental data are shown as solid circles and triangles.

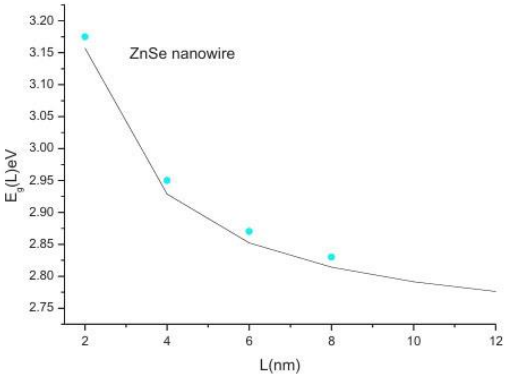

Figure.11 The energy band gap of ZnSe nanowires varies with size. A continuous line shows the values estimated in this research using Equation (10) while solid circles and triangles indicate the experimental data.

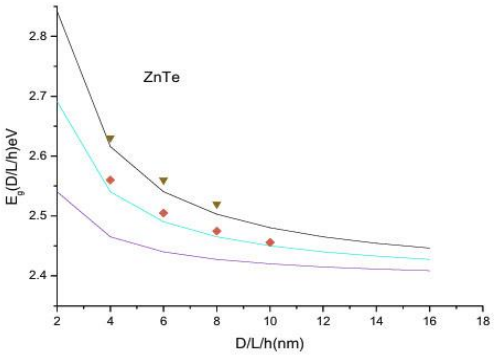

Figure.12 Energy band gap changes in ZnTe nanospheres, nanowires, and nanofilms with size. The continuous line shows Equations (9)– (11) values, whereas the solid delta and square reflect experimental findings.

Figure 12 shows that as we go from spherical to nanowire and nanofilm, the influence of size diminishes. Given that the surface to volume ratio rises with decreasing size, this pattern is predicted. It should be noted that the CdSe, CdTe, ZnS, ZnSe, and ZnTe nanofilms do not yet have access to the experimental findings. For the time being, we are publishing our model forecast without any experimental data. Our forecast could now be of interest to researchers doing experimental investigation. Since cohesive energy reduces by Equation (3) as nanofilm particle size decreases, this causes a rise in band gap energy, which is initiated by Equation (11). Figure 4 displays the size dependence of the CdTe nanosphere's band gap energy using Equation (9). It is observed that when the particle size decreases, the CdTe nanosphere's band gap energy rises. The published findings are contrasted with the experimental observations that are at hand. The experiments and our suggested model agree rather well. Figure 5 shows the size dependence of the CdTe nanowire's band gap energy using Equation (10). We contrasted the experimental results published by Li et al. with our predictions. It has been found that the energy band gap fluctuation follows a similar pattern. For sizes lower than 5 nm, there is a good agreement between known experimental evidence and theory. Figures 7–8 reveal variations in energy band gaps and experimental results for ZnS nanomaterials in nanosphere and nanowire geometries with sizes. This demonstrates that the formulation used was accurate. We have computed the band gap of ZnSe nanomaterial semiconductor in various sizes and shapes using Equations (9) and (10). Figures 10 and 11 report the calculated values. The experimental results are in good agreement with our model predictions. There is a good agreement with the experiment for ZnSe nanosphere over its whole size range. The size dependence of ZnSe nanowire's band gap growth is seen in Figure 11. The resulting outcomes are contrasted with the data from the experiment. The band gap expansion grows slowly at first and then quickly as the size decreases, as the image illustrates. A graphical representation of the growth in band energy with size and form demonstrates that, at the nanoscale, shape is just as important as size. Shape and size affect the volume to surface area ratio, which in turn affects the cohesive energy and the number of surface atoms at the nanoscale. Thus, at the nanoscale, the band gap energy varies. This may be explained quantum mechanically as the number of overlapping orbitals or energy levels drops and the band width thins as the particle size approaches the nanoscale. The energy band gap between the valence band and the conduction band will increase as a result. This explains why SCNs have a larger energy band gap than their bulk equivalent.

4. Conclusion

An elementary model is developed to compute the band gap energy of semiconductor nanomaterials of various sizes and forms, including spherical nanospheres, nanowires, and nanofilms. The hypothesis states that the energy band gap of semiconductor nanoparticles grows as the particle size of the nanomaterials decreases. Moreover, our computer model accurately predicts the energy band gap, which is in good agreement with the existing experimental results. We are certain that this theory will play a significant role in applications where experimental evidence is now unavailable.

Reference

[1] Brenner, Sara A., et al. "Occupational exposure to airborne nanomaterials: an assessment of worker exposure to aerosolized metal oxide nanoparticles in semiconductor wastewater treatment." *Journal of occupational and environmental hygiene* 12.7 (2015): 469-481.

[2] Shepard, Michele Noble, and Sara Brenner. "An occupational exposure assessment for engineered nanoparticles used in semiconductor fabrication." *Annals of occupational hygiene* 58.2 (2014): 251-265.

[3] Jakka, Geethamanikanta, N. S. L. K. Kanulla, and Oludotun Oni. "Analysing The Need Of Big Data Owners To Regularly Update Security Measures." *Journal of Pharmaceutical Negative Results* (2022): 8417-8425.

[4] Warheit, David B., et al. "Testing strategies to establish the safety of nanomaterials: conclusions of an ECETOC workshop." *Inhalation toxicology* 19.8 (2007): 631-643.

[5] V. K. Chidipothu, L. k. Kanulla, C. K. Pandey, S. K. Davuluri, M. Tiwari and D. P. Singh, "Design and Implementation of Block Chain with Cybersecurity Scheme for Fog Based Internet of Things," *2023 6th International Conference on Contemporary Computing and Informatics (IC3I)*, Gautam Buddha Nagar, India, 2023, pp. 1409-1415, doi: 10.1109/IC3I59117.2023.10397622

[6] Aggarwal, Anil Kr, Sanjeev Kumar, and Vikram Singh. "Mathematical modeling and reliability analysis of the serial processes in feeding system of a sugar plant." *International Journal of System Assurance Engineering and Management* 8 (2017): 435-450.

[7] Boyd, Robert D., et al. "Good practice guide for the determination of the size distributions of spherical nanoparticle samples." (2011).

[8] BramahHazela, et al. "Machine Learning: Supervised Algorithms to Determine the Defect in High-Precision Foundry Operation." *Journal of Nanomaterials* 2022.1 (2022): 1732441.

[9] Song, Woo-Young, Seung-Soo Lee, and Yong-Jun Kim. "Airborne nanoparticle analysis mini-system using a parallel-type inertial impaction technique for real-time monitoring size distribution and effective density." *Sensors and Actuators A: Physical* 341 (2022): 113591.

[10] BramahHazela, et al. "Machine Learning: Supervised Algorithms to Determine the Defect in High-Precision Foundry Operation." *Journal of Nanomaterials* 2022.1 (2022): 1732441.

[11] Svensson, C. R., et al. "Validation of an air–liquid interface toxicological set-up using Cu, Pd, and Ag well-characterized nanostructured aggregates and spheres." *Journal of Nanoparticle Research* 18 (2016): 1-20.

[12] Kwak, Dongbin. *Fundamental Study of Particle Formation, Transport, Deposition and Filtration for Semiconductor Applications*. Diss. University of Minnesota, 2023.

[13] G. Laxmaiah, S. S. Raj, T. R. Kumar and R. M. M. Shareef, "Experimental and Simulation analysis of Monitoring a Industrial process by Adaptive transfer Learning," *2023 International Conference on New Frontiers in Communication, Automation, Management and Security (ICCAMS)*, Bangalore, India, 2023, pp. 1-7, doi: 10.1109/ICCAMS60113.2023.10526180.

[14] Frank, Uwe, et al. "Progress in multidimensional particle characterization." *KONA Powder and Particle Journal* 39 (2022): 3-28.

[15] Kumar, T. Rajasanthosh, et al. "Implementation of Intelligent CPS for Integrating the Industry and Manufacturing Process." *AI-Driven IoT Systems for Industry 4.0*. CRC Press, 2024. 273-288.

[16] Jensen, Keld A., and François Gensdarmes. "SESSION II INSTRUMENTATION, CHARACTERIZATION & EXPOSURE EVALUATION." *Dear Participants* 21.s1 (2011): 59.

[17] Stone, Vicki, et al. "Nanomaterials versus ambient ultrafine particles: an opportunity to exchange toxicology knowledge." *Environmental health perspectives* 125.10 (2017): 106002.

[18] Hess, Adrian, Mohamed Tarik, and Christian Ludwig. "A hyphenated smps–icpms coupling setup: Size-resolved element specific analysis of airborne nanoparticles." *Journal of Aerosol Science* 88 (2015): 109-118.

[19] Sob, Peter Baonhe. *Modelling stain rate sensitive nanomaterials' mechanical properties: the effects of varying definitions*. Diss. 2016.

[20] Zuin, Stefano, Giulio Pojana, and Antonio Marcomini. "Effect-oriented physicochemical characterization of nanomaterials." *Nanotoxicology*. CRC Press, 2007. 35-74.

[21] Lee, Handol, et al. "Effects of filter structure, flow velocity, particle concentration and fouling on the retention efficiency of ultrafiltration for sub-20 nm gold nanoparticles." *Separation and Purification Technology* 241 (2020): 116689.

[22] Kwon, Hong-Beom, et al. "Monitoring the effective density of airborne nanoparticles in real time using a microfluidic nanoparticle analysis chip." *ACS sensors* 6.1 (2021): 137-147.

[23] Todea, Ana Maria, et al. "Development of a method to determine the fractional deposition efficiency of full-scale hvac and hepa filter cassettes for nanoparticles≥ 3.5 nm." *Atmosphere* 11.11 (2020): 1191.

[24] Zazzera, Larry, et al. "Comparison of ceria nanoparticle concentrations in effluent from chemical mechanical polishing of silicon dioxide." *Environmental science & technology* 48.22 (2014): 13427-13433.

[25] Meierhofer, Florian, and Udo Fritsching. "Synthesis of metal oxide nanoparticles in flame sprays: review on process technology, modeling, and diagnostics." *Energy & Fuels* 35.7 (2021): 5495-5537.